

# Sensing the distance to a source of periodic oscillations in a nonlinear chemical medium with the output information coded in frequency of excitation pulses

J. Gorecki,<sup>1</sup> J. N. Gorecka,<sup>2</sup> K. Yoshikawa,<sup>3</sup> Y. Igarashi,<sup>3</sup> and H. Nagahara<sup>3</sup>

<sup>1</sup>*Institute of Physical Chemistry, Polish Academy of Science, Kasprzaka 44/52, 01-224 Warsaw, Poland*  
and *Faculty of Mathematics and Natural Sciences, Cardinal Stefan Wyszyński University, Dewajtis 5, 01-815 Warsaw, Poland*

<sup>2</sup>*Institute of Physics, Polish Academy of Sciences, Al. Lotników 36/42, 02-668 Warsaw, Poland*

<sup>3</sup>*Department of Physics, Graduate School of Science, Kyoto University, Kyoto 606-8502, Japan*

(Received 9 May 2005; published 3 October 2005)

A spatially distributed excitable chemical medium can collect and process information coded in the propagating pulses of excitation. We consider the problem of distance sensing with the use of a nonlinear chemical medium. We demonstrate that a sensor that can feel the distance separating it from a source of periodic excitations can be constructed by a proper geometrical arrangement of excitable and nonexcitable regions. The sensor returns information about the distance in the frequency of outgoing pulses. The sensor functionality is tested by simulations based on the Rovinsky-Zhabotinsky model. The results are confirmed in experiments performed for a ruthenium-catalyzed Belousov-Zhabotinsky reaction.

DOI: [10.1103/PhysRevE.72.046201](https://doi.org/10.1103/PhysRevE.72.046201)

PACS number(s): 05.45.-a, 89.75.Kd, 82.40.Ck

## I. INTRODUCTION

A spatially distributed chemical reaction-diffusion system can work as an information processing medium in which information is coded in pulses of excitation [1–4]. The way in which such a system transforms information depends on its geometrical structure and the properties of reactions involved. The information processing in an chemical excitable medium can be different from the von Neumann architecture [5] commonly used in computers, where an external clock fixes the sequence of operations that are executed. It is believed that excitable media play a crucial role in information processing in living organisms [6].

Exploring the environment for the optimum living conditions and resources of food is one of the most important problems a living organism should solve. Animals like bats or owls use wave-related effects (intensity, frequency, or delay of sound) to get information on the location of a prey [7]. It is expected that in the case of very simple organisms like bacteria sensing the environment is based on chemical processes occurring in a cell. Therefore, we believe that research on chemical aspects of sensing can help in better understanding living organisms. In this paper we describe how a nonlinear chemical medium can be applied for distance sensing. We demonstrate that using a chemical system with a properly defined geometry of excitable (active) and nonexcitable (passive) regions one can construct a device that can sense the distance separating it from a source of periodic excitations. The information on the distance between the source of excitations and the observer is coded in the frequency of signals sent through a number of channels.

The approach presented in this paper is an alternative to the method of chemical sensing recently discussed by Nagahara *et al.* [8]. The sensor of direction of a chemical wave described in [8] used the coincidence of pulses to recognize the direction of a single excitation coming to an observer. The sensor was formed by a ring of an excitable medium and a number of coincidence detectors placed around it. An ar-

iving excitation generates two pulses on a ring that propagate in opposite directions. The coincidence detector located near the point at which the generated pulses meet becomes excited. Of course, the position of the meeting point depends on the wave vector of the arriving excitation. Therefore, the system presented in [8] returns information about the direction of excitation in the form of a pulse propagating in an appropriate channel.

In this paper we demonstrate an alternative method of sensing that may be used in an excitable chemical medium. It is based on the transformation of the frequency of periodic excitations and returns the information in the form of pulses propagating in a number of channels. We show that the idea of sensing based on frequency transformation of chemical signals can be applied to detect the distance from the source of a periodic train of excitations. The considered sensor of distance is investigated using numerical simulations for the model of an excitable medium with the ferroine-catalyzed Belousov-Zhabotinsky (BZ) reaction and in the experiments with a Ru-catalyzed BZ reaction. In both cases we demonstrate that the frequency of excitations in the sensor channels gives the information on the distance from the source.

## II. DISTANCE SENSOR

The amplitude of peaks in a periodic train of autowaves in an excitable system is a function of their frequency. It is known [9–13] that a passive barrier can transform the signal frequency. As expected, the frequency of a periodic signal transmitted through a barrier increases with the strength of excitation behind the barrier generated by a single arriving pulse. For a given frequency of excitations arriving at a barrier (and so for a given amplitude of excitations) the frequency of excitations behind the barrier is regulated by the barrier width and the angle between the normal to the barrier and the wave vector of the arriving pulse. The geometrical arrangement of active and passive areas in the proposed chemical distance sensor is shown in Fig. 1. Let us consider

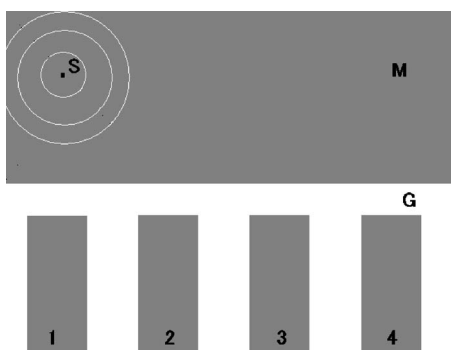


FIG. 1. The geometry of a chemical distance sensor. The gray areas are excitable; the white areas are nonexcitable. The source of excitations,  $S$ , is marked by a black dot.

an active medium  $M$ . The source of excitations,  $S$ , is placed within the medium. The source generates a train of excitations, and at very short distances the shape of pulses reflects the source geometry. The idea of a device that can sense the distance separating it from the source of excitations can be described in the following way. Let us consider a number of similar excitable signal channels (in Fig. 1 they are numbered 1–4) that are wide enough to ensure a stable propagation of pulses. These signal channels (we call them sensor channels) are separated one from another by parallel nonexcitable gaps that do not allow for interference between pulses propagating in the neighboring channels. The sensor channels are separated from the active medium  $M$  by a nonexcitable sensor gap  $G$ . The width of this gap is crucial for sensor sensitivity. If the gap is too wide, then no excitation of the medium  $M$  can generate a pulse in the sensor channels (1–4). If the gap is narrow, then any excitation in front of a sensor channel can pass  $G$  and create a pulse in the channel, so the signals in every sensor channel are identical. The width of the gap should be selected such that the firing number (defined as the ratio between the number of pulses that crossed the gap  $G$  to the number of pulses of excitation that were created in the medium  $M$ ) depends on the wave vector characterizing a pulse at the gap in front of the channel. It is also very important that the gaps between the active area  $M$  and each channel are exactly the same.

If the source  $S$  is close to the array of sensor channels, then the wave vectors characterizing excitations in front of various channels will be different. Thus we expect different frequencies of excitations in various channels. On the other hand, if the source of excitations is far away from the gap  $G$ , then the wave vectors in front of different channels should be almost identical and so the frequencies of excitations in different channels would not differ. Therefore, the system shown in Fig. 1 can sense the distance separating it from the source of excitations. If this distance is small, the firing numbers in neighboring sensor channels are different and these differences decrease when the source of excitations moves away.

### III. SIMULATIONS AND EXPERIMENTAL STUDIES OF THE DISTANCE SENSOR

In this section we present results of simulations and experiments that demonstrate that the distance sensor illus-

trated in Fig. 1 works. We discuss the range of distances in which sensing is effective and the influence of the geometry of sensor on its sensitivity.

In our numerical simulations we have used a well-known, simple Rovinsky-Zhabotinsky (RZ) model of a ferroin-catalyzed BZ reaction [14,15]. The RZ model uses two variables  $x$  and  $z$ , corresponding to the dimensionless concentrations of the activator  $\text{HBrO}_2$  and of the oxidized form of catalyst  $\text{Fe}(\text{phen})_3^{3+}$ . In the active regions the time evolution of the concentrations of  $x$  and  $z$  is described by

$$\frac{\partial x}{\partial \tau} = \frac{1}{\epsilon} \left[ x(1-x) - \left( 2q\alpha \frac{z}{1-z} + \beta \right) \frac{x-\mu}{x+\mu} \right] + \nabla_{\rho}^2 x, \quad (1)$$

$$\frac{\partial z}{\partial \tau} = x - \alpha \frac{z}{1-z}. \quad (2)$$

The passive regions are areas of space where the catalyst is absent, so  $z=0$ , and the evolution of  $x$  is described by

$$\frac{\partial x}{\partial \tau} = -\frac{1}{\epsilon} \left[ x^2 + \beta \frac{x-\mu}{x+\mu} \right] + \nabla_{\rho}^2 x. \quad (3)$$

All variables and coefficients in Eqs. (1)–(3) are dimensionless and the real concentrations of  $\text{HBrO}_2$  and  $\text{Fe}(\text{phen})_3^{3+}$  ( $X, Z$ ) are related to  $(x, z)$  in the following way:  $X = (k_1 A / 2k_4) x$  and  $Z = Cz$  where  $k_{\pm i}$  denote the rate constants of the corresponding reactions in the Field-Körös-Noyes model [14,15],  $A = [\text{HBrO}_3]$ , and  $C = [\text{Fe}(\text{phen})_3^{2+}] + [\text{Fe}(\text{phen})_3^{3+}]$ . The coefficients  $\alpha$ ,  $\beta$ ,  $\mu$ , and  $\epsilon$  are defined in [15,16]. In numerical calculations we use the values of  $\alpha$ ,  $\beta$ ,  $\epsilon$ , and  $\mu$  equal to  $0.017h_0^{-2}$ ,  $0.0017h_0^{-1}$ ,  $0.1176$ , and  $0.00051$ , respectively and  $h_0 = 0.5$  [14–16]. For the values of parameters defined above the stationary concentrations of  $x$  and  $z$  in the active area are  $x_{sa} = 7.283 \times 10^{-4}$  and  $z_{sa} = 1.060 \times 10^{-2}$  and the stationary value of  $x$  in the passive area is  $x_{sp} = 5.10 \times 10^{-4}$ .

The relationships between dimensionless time  $\tau$  and distance  $\rho$  used in Eqs. (1)–(3) and the real time  $t$  and distance  $r$  are the following:

$$t = \frac{k_4 C}{k_1^2 A^2 h_0} \tau, \quad (4)$$

$$r = \sqrt{\frac{k_4 C}{h_0}} \frac{1}{k_1 A} \sqrt{D_X} \rho, \quad (5)$$

where  $D_X$  is the diffusion constant of the activator  $x$ . For the parameters chosen,

$$t[\text{sec}] = 8.5\tau, \quad (6)$$

and for a typical diffusion of reagents in aqueous solution  $D_X = 1 \times 10^{-5} \text{ cm}^2/\text{sec}$  [15,17],

$$r[\text{mm}] = 9.218 \times 10^{-2} \rho. \quad (7)$$

Equations (1)–(3) correspond to a typical experimental situation in which ferroin is immobilized on a flat membrane, whereas the activator is in the solution and it can

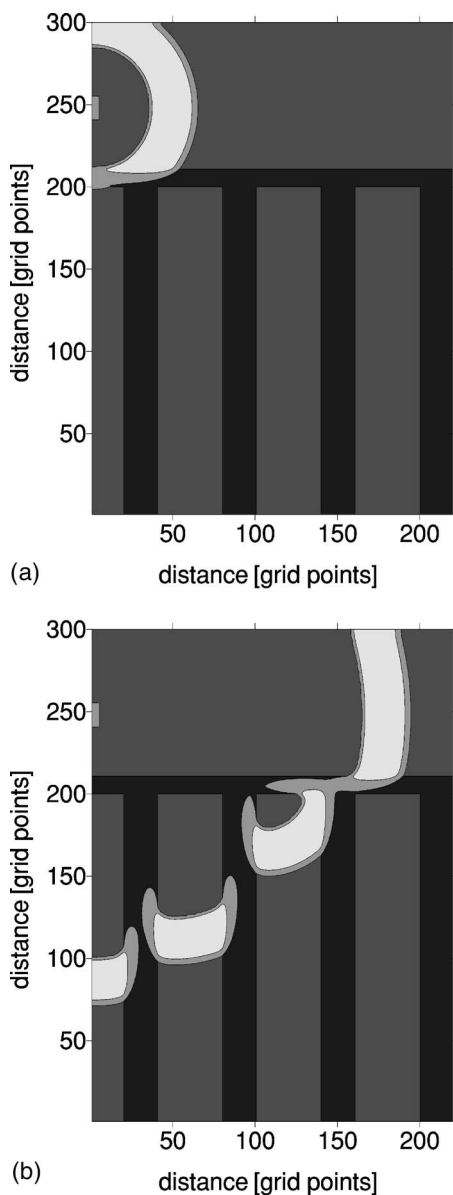


FIG. 2. Two typical snapshots from simulations. The gray areas are excitable; the black areas are nonexcitable. The source of excitations is marked as a light area close to the *OY* axis around 250. The light color shows the profile of a high concentration of *x* for times  $\tau=4$  (a) and  $\tau=12$  (b). The *x*- and *y*-axis scales are grid points.

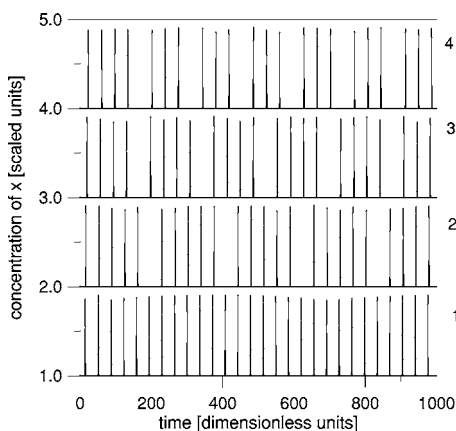
diffuse (compare [17,18]). Therefore, it is natural to consider free-boundary conditions between the active and passive areas.

The reaction-diffusion equations (1)–(3) for the distribution of active and passive areas shown in Fig. 2 are solved on a grid of points equally distant in the *x* and *y* directions ( $\Delta x = \Delta y = 0.2885$ ). The calculations are performed using the explicit Euler algorithm for the diffusion combined with the fourth-order Runge-Kutta method for the chemical kinetics and the time step  $\Delta\tau=0.001$ . The number of grid points in the *x* direction (220) was the same in all simulations. The left active channel (channel No. 1) was 20 grid points wide whereas all the other channels were 40 points wide. The

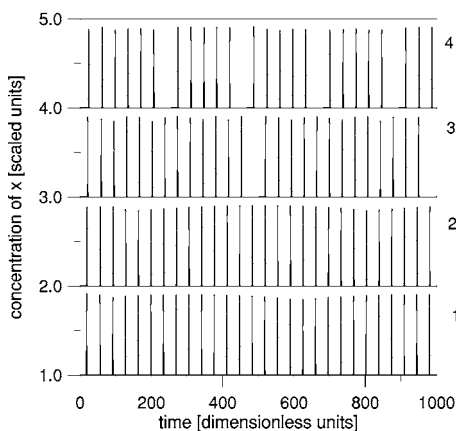
difference is related to the no-flux boundary conditions used. Such boundary conditions force the symmetry with respect to the vertical axis, and thus the actual width of the channel below the source is the same as the width of the other channels. The passive stripes separating the sensor channels are 20 grid points wide (5.77 in dimensionless distance units) and the sensor channels are 200 grid points long (57.7 distance units). The number of grid points along the *y* direction depends on the distance between the source of excitations, *S*, and the detector. Usually the size of grid is such that there are over 50 grid points corresponding to the active medium above the upper boundary of the source.

The initial values of *x* and *z* in the active areas and *x* in the passive regions correspond to the stationary values  $x_{sa}$ ,  $z_{sa}$ , and  $x_{sp}$ , respectively. At the beginning of simulations these values change slightly near the boundaries due to diffusion between active and passive areas, but the system approaches its stable, stationary state within a very short time. The source of periodic excitations is realized as an area of space with a high concentration of activators, which remains constant in the simulations. The frequency of pulses outgoing from such a center of excitations depends on both the size of the source and the assumed concentration of activators. The considered source of excitations corresponds to the experimental situation where the tip of a silver wire is permanently placed in the active medium and works as the continuous source of a train of spherical pulses. The source of excitations is marked in Fig. 2 as the light area on the vertical axis near 250.

As expected, the width of the passive gap separating the active medium *M* from the sensor channels is crucial for the sensor work. The results shown in Fig. 2 have been obtained for a gap 10 grid point wide ( $\Delta_G=2.885$ ). In the presented case the source of excitations was 5 grid points wide and 15 grid points high ( $1.4425 \times 4.3275$  distance units). The concentration of activators in the source region was 0.02. For such size and concentrations the period of excitations was 34.8. Figures 2(a) and 2(b) show two typical snapshots from simulations for the source placed close to the detector. It is easy to see that the shapes of an excitation pulse in the active medium in front of various sensor channels are different. The shape of the excitation pulse in front of a given sensor channel depends on the distance between the source and sensor. The differences in shape lead to different strengths of excitations behind the barriers and finally translate into various frequencies of pulses in sensor channels. The time evolution of the concentration at points centrally located within the channels 1, 2, 3, and 4 is shown in Fig. 3. Figures 3(a) and 3(b) present results for the system illustrated in Fig. 2 and two different distances between the source of excitations and the detector. They correspond to situations where the distance is short [5.77, Fig. 3(a)] and where the distance is long [25.97, Fig. 3(b)]. As expected, the frequency in the channel below the source is the largest because the arriving pulse is normal to the sensor gap and it does not depend on the distance between the source and sensor. It is clearly seen that for a short distance the frequencies of pulses in sensor channels 1–4 are significantly different, whereas if the distance between the source and sensor is long, the frequencies are almost the same. The conclusion that the distance separating



(a)



(b)

FIG. 3. (a) and (b) show the concentration of  $x$  in channels 1, 2, 3, and 4 as functions of time for the system presented in Fig. 2. (a) and (b) correspond to the distances between the source and detector gap equal to 5.77 and 25.97, respectively. The concentrations are shifted vertically by a value equal to the number of channels.

the source from the detector can be obtained from the set of firing numbers in sensor channels if the results presented in Fig. 4, which show the firing numbers as functions of distance. The firing number in channels 1, 2, 3, and 4 for the barrier width  $\Delta_G=2.885$  and concentration of the activator in the source equal to 0.02 are marked by dots, triangles, squares, and crosses, respectively. All simulation runs were carried for more than 5000 time units, which allowed for a precise measurements of the firing number in all detector channels. It can be seen that knowledge of all firing numbers gives a precise estimation of the distance between the detector and source.

Having in mind that the signal transformation on a barrier depends on the frequency of incoming pulses [9,10] we should consider if this phenomenon influences the work of the distance sensor. In order to study the effect we performed simulations for another source of excitations that occupies a larger area of space ( $10 \times 15$  grid points), but the concentration of activator in the source is significantly reduced (0.015). The excitation is weaker, and so the medium requires a longer relaxation time before it can be excited again. For the parameters described above the period of excitations

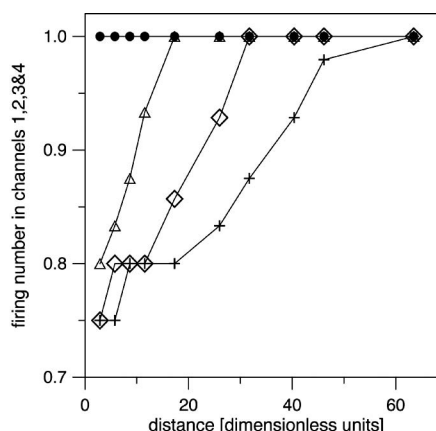


FIG. 4. The firing number in channels 1 (dots), 2 (triangles), 3 (squares), and 4 (crosses) as a function of distance; the barrier width  $\Delta_G=2.885$ , excitation at the level 0.02.

is 61 time units. It comes out that the sensor with  $\Delta_G=2.885$  described above does not work because for a lower frequency of excitations the firing numbers in all channels are equal to 1 regardless of the source position. However, if the width of the gap increases, the sensor works again. Figure 5 shows results for ( $\Delta_G=3.2$ , ten grid points with grid step  $\Delta=0.32$ ). Now within a range of distances separating the sensor from the source the firing numbers in different channels are different and estimation of distance becomes possible again. Therefore the described chemical sensor of distance requires a method of adaptation to the conditions it operates. In practice, such an adaptation can be realized by a comparison of frequencies of signals in detector channels with the frequency in a control channel. The control channel is separated from the medium  $M$  by a barrier that is so narrow that every excitation of the medium is transmitted. The comparison between the frequency of excitations in the control channel and in the sensor channels can be used to adjust  $\Delta_G$ . If the frequency of excitations in the sensor channels is the same as in the control channel, then the gap should be increased. On the other hand, if the frequency in the sensor

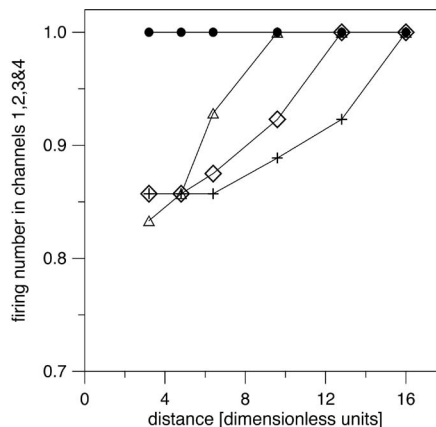


FIG. 5. The firing number in channels 1 (dots), 2 (triangles), 3 (squares), and 4 (crosses) as a function of distance; the barrier width  $\Delta_G=3.2$ , excitation at the level 0.015.



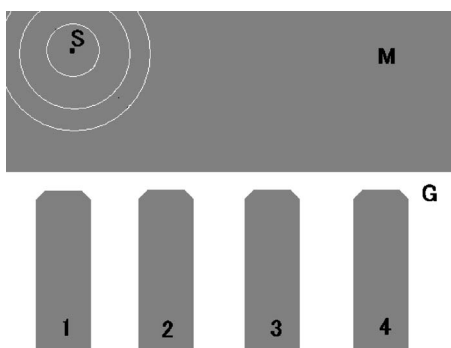


FIG. 6. The chemical distance sensor with a modified geometry. Like in Fig. 1 the gray areas are excitable and the white areas are nonexcitable. The source of excitations,  $S$ , is marked by a black dot.  $\Delta_G=2.9$ .

channel is much smaller than in the control channel (or null), then  $\Delta_G$  should be decreased. Allowing for such a mechanism of adaptation one can construct a device that works for any frequency of arriving excitations.

From Fig. 2(b) it is clear that the wavelength of a pulse ( $\lambda$ ) is longer than 55 distance units. Comparison between the firing number as a function of distance and the wavelength (Fig. 4) shows that the sensor can recognize distances much shorter than  $\lambda$  with the precision at the level of a few percent. These results also show (Figs. 4 and 5) that within the range of distances that can be recognized the changes in the firing numbers are very limited. Simulations indicate that the range of firing numbers observed in sensor channels can be extended if the geometry of the tip of the sensor channel is modified. An alternative geometry of the distance sensor is shown in Fig. 6. The firing number as a function of the distance for the sensor with the modified geometry is shown in Fig. 7. Here the source of excitations was  $5 \times 15$  grid points large and the concentration of activators in the source was equal to 0.02 (so the source was the same as used with the "normal" sensor shown in Fig. 2). The calculations were performed for ( $\Delta=0.29$ ) and the minimum width of the sensor gap was ten grid points ( $\Delta_G=2.9$ ). The working range of

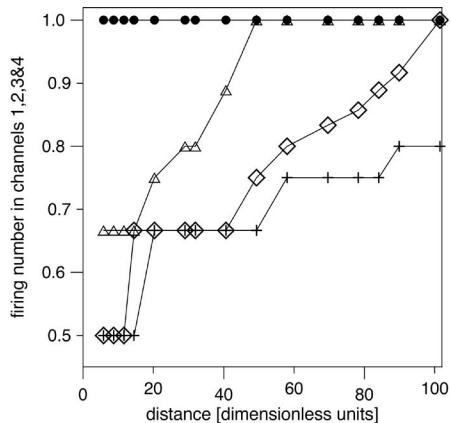


FIG. 7. The firing number in channels 1 (dots), 2 (triangles), 3 (squares), and 4 (crosses) as a function of distance for the detector with a modified geometry ( $\Delta_G=2.9$ ).

distances for which the modified sensor operates has been significantly increased, and the answer is more precise. This observation opens the question on the optimal shape of the sensor channel for the distance sensing.

Although in simulations we have used the kinetics equations for the system with a ferroine-catalyzed BZ reaction, the results describe the most essential features of the experiment with the ruthenium catalyst. It is, thus, clear that the informational processing on distance sensing is performed not only through numerical simulation but also through a real experiment.

The experimental results were obtained with a photosensitive Ru-catalyzed BZ reaction. The reaction was studied on cellulose-nitrate membrane filters (A100A025A, 2.5 cm diameter, Advantec) with a pore size of 1.0  $\mu\text{m}$ . The membrane was soaked for 4 min in the following solution of BZ reagents: 1 ml of  $\text{NaBrO}_3$  (1.5 mol), 0.25 ml of  $\text{H}_2\text{SO}_4$  (3.0 mol), 0.5 ml of  $\text{CH}_2(\text{COOH})_2$  (1.0 mol), 0.125 ml of  $\text{KBr}$  (1 m), 0.5 ml of  $\text{Ru}(\text{bpy})_3\text{Cl}_2$  (8.5 mmol) (all reagent-grade chemicals from Wako Pure Chemicals, Japan), and 0.125 ml of doubly distilled water. After having been soaked, the membrane was gently wiped to remove excess solution (we used a wipe tissue made by Kimwipe), placed in a Petri dish, and immediately covered with silicone oil (Shin-Etsu Chemical Co.) to prevent it from drying and to protect it from the influence of oxygen. The room temperature was  $23 \pm 1$   $^\circ\text{C}$ . The geometrical distribution of active and passive regions was introduced by illumination. The experimental setup was the same as described in [19] with the only difference that a liquid-crystal projector (Epson ELP-810) attached to a computer was used as a light source. The position of the sensor gap and the sensor channels were generated as a graphic file. This graphic file was displayed on a membrane filled with the reagents of the BZ reaction. The light intensity was selected such that nonilluminated parts of the membrane were excitable, whereas the excitations died in the illuminated areas. The light intensity measured with light meter (ASONE LM-332) was  $26.5 \times 10^4$  lx in the illuminated areas and  $0.3 \times 10^3$  lx in nonilluminated ones. The medium  $M$  was over 15 mm  $\times$  15 mm large. The detector channels were 1 mm wide. The gap between the signal area and detector channels was 0.5 mm whereas the gaps between detector channels were 0.9 mm wide. The train of excitations was generated by a tip of a silver wire (1 mm thick) that was permanently placed in a selected place on the membrane. The propagation of pulses was recorded with a digital video camera (Panasonic NV-DJ100) and analyzed using standard image processing techniques. For the image enhancement, a blue optical filter (AsahiTechnoGlass V-42) with a maximum transparency of 410 nm was used. Typical snapshots from two experiments performed for the source placed 2 and 12 mm away from the sensors are shown in Fig. 8. The observed firing numbers are given next to the corresponding sensor channels. The results allow us to estimate the sensor range. In the case when the source of excitations is away from the sensor the angle between lines pointing towards the centers of two nearest channels is 0.16 rad. This difference of angle corresponds to a noticeable change in the observed firing numbers (0.484 vs 0.451). A similar difference between firing numbers in the side signal channels should be

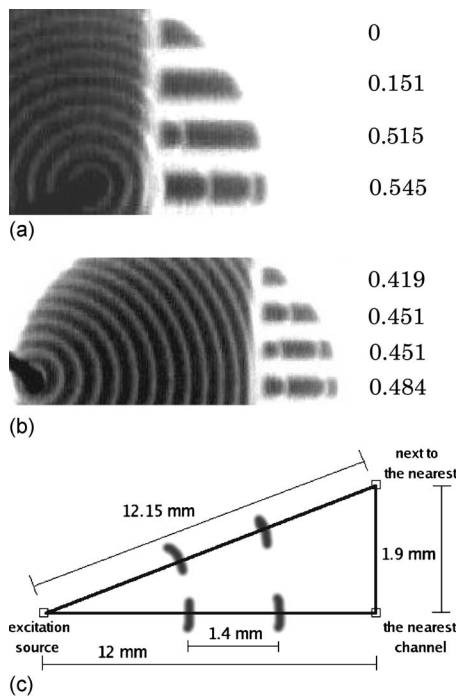


FIG. 8. (a) and (b) are snapshots from the experimental realization of the distance sensor. The upper figure shows the source (1-mm-thick silver wire) placed 2 mm away from the sensor; in the lower one the source was 12 mm away. The firing numbers are given next to the corresponding channels. (c) The distances between centers of signal channels and the distance source.

observed if the source is around 3 cm away from the sensor [see Fig. 8(c)], so the useful range of distances at which our sensor works is measured in centimeters.

The firing numbers observed in different sensor channels confirm qualitatively the predictions of numerical simulations. If the source of excitations is close to the sensor gap, the differences between firing numbers observed in neighboring channels are large. On the other hand, when the source of excitations is far away from the sensor the frequencies in different channels become similar.

#### IV. CONCLUSIONS

In this paper we discussed the application of an excitable chemical medium for the estimation of distance separating an observer from a source of periodic excitations. We have demonstrated that by setting a proper geometrical arrangement of excitable and nonexcitable regions one can construct a device that can sense the distance from the source. We considered two-dimensional sensors only but the same idea may be applied to three dimensions if the channels are represented by cylindrical tubes. The information about the distance is returned in the firing numbers of excitations in a set of sensor channels. If the source is placed close to the sensor, then large differences between firing numbers in the neighboring sensor channels are observed. When the source is far away from the sensor, the frequencies in all sensor channels are the same. The numerical simulations have revealed inter-

esting properties of the sensor of distance. For example, its characteristics depend on the width of sensor gap separating channels from the active medium. To obtain the optimum sensitivity the gap width should be adjusted depending on the period of excitations. Moreover, we have demonstrated that the shape of the junction separating sensor channels from the excitable medium has an important effect on the range and accuracy.

Knowing the firing numbers in all channels we can estimate the distance from the source (see Figs. 4 and 7 showing the results for four channel sensors). However, it would be difficult to give an analytical formula linking the set of firing numbers with distance or to estimate the error. It is known (see, for example, Fig. 1 in [9]) that the dependence of firing number on the stimulus strength has a devil's-staircase-like form and long intervals where the function is constant correspond to simple fractions. Here, such a devil's-staircase-like function describes the firing number in a separate channel as a function of source distance (cf. Figs. 4 and 7). In the case of a modified four-channel sensor (Fig. 7) there are some intervals of distances that correspond to the same set of firing numbers [for example, distances between 5 and 11.6 correspond to the set  $(1, 2/3, 1/2, 1/2)$ ] so the resolution in this range of distances is poor. On the other hand, the sensor can easily discriminate the change in source distance from 11.6 to 14.5 because the set of firing numbers changes into  $(1, 2/3, 2/3, 1/2)$ . Thus the resolution of a sensor depends on how the constant pieces of devil's-staircase-like firing numbers in separate channels as a function of source distance overlap. A few strategies for error reduction can be easily proposed. We can increase the number of sensor channels so the overlaps are less probable. Alternatively we can use two sensors with different gaps working in parallel and combining their results. For example, the normal sensor with the characteristics shown in Fig. 4 increases the resolution of the modified sensor (Fig. 7) at short distances.

Both in experiments and in simulations we considered the case when a source of oscillations is above one of the sensor channels. In such a case the sensor can recognize the projection of the source position on the line parallel to the sensor gap (the  $X$  axis in Fig. 2) because the maximum firing number is observed in the channel below the source. The sensor can also estimate the distance to a source placed in the excitable medium not above any channel. In such a case the maximum firing number is observed in a side channel that is the closest to the source. Like in the studied case the same firing number in sensor channels indicates that the source is far away for the sensor, whereas large differences between firing numbers show that the source is close.

In the experiments and simulations discussed above we assumed that the same dynamics describes the excitable medium  $M$  and the sensor channels. Such an assumption is not necessary and the excitabilities of the medium and of the channels may differ. The same sensor can operate in various media (an analogy with bacteria in different environments) if it is equipped with the mechanism of adaptation that controls the gap width according to the strength of excitations coming from the medium as described in Sec. III.

The presented sensor can be also used to trace the motion of the source of excitations. If the differences in the firing

numbers observed in sensor channels are increasing, then the source comes closer to the detector. Contrary, if the frequencies of excitations in the channels become similar, then the source of excitations moves away. Of course, the speed of the source should be much smaller than the velocity of excitation pulse. In this paper we calculated firing numbers in long simulations covering hundreds of periods, but in practice the observation of an output signal for time that is ten periods long seems sufficient to recognize firing number  $1/2$ ,  $2/3$ , or  $3/4$ . Such firing numbers correspond to a source placed close to the observer and information on source motion seems to be more important than in the case where the source is far away. In the case of the modified sensor (Fig. 7) the change of firing number from  $3/4$  to  $1/2$  corresponds to the change of distance by 40 units. It means that motion of the source with velocity of the order of 1% of the pulse velocity can be detected.

We believe that the described distance sensor has many features that characterize sensing in biological systems like the accommodation mechanism for optimal performance or the output information coded in the frequency of pulses. It is known that the channels in nonexcitable membranes can transform the frequency of excitations [20], and so they can play a role similar to the sensor gap in the sensor discussed here. Therefore, it seems worthwhile to study analogies between chemical sensing and processes in simple living organisms.

#### ACKNOWLEDGMENTS

This research was supported by the Polish-Japanese joint research project "Information processing in excitable chemical systems" and the Polish State Committee for Scientific Research Project No. 1 P03B 035 27.

- 
- [1] I. N. Motoike and K. Yoshikawa, *Phys. Rev. E* **59**, 5354 (1999).
- [2] S. Nakata, *Chemical Analysis Based on Nonlinearity* (Nova Science, New York, 2003).
- [3] N. Rambidi, *BioSystems* **64**, 169 (2002).
- [4] A. Adamatzky, B. de Lacy Costello, and N. M. Ratcliffe, *Phys. Lett. A* **297**, 344 (2002).
- [5] R. P. Feynman, R. W. Allen, and T. Heywood, *Feynman Lectures on Computation* (Addison-Wesley, Reading, MA, 1996).
- [6] H. Haken, *Brain Dynamics*, Springer Series in Synergetics (Springer-Verlag, Berlin, 2002).
- [7] A. Moiseff and T. Haresign, in *Nature Encyclopedia of Life Sciences*, <http://www.els.net>
- [8] H. Nagahara, T. Ichino, and K. Yoshikawa, *Phys. Rev. E* **70**, 036221 (2004).
- [9] J. Siewleskiuk and J. Gorecki, *Phys. Rev. E* **66**, 016212 (2002).
- [10] J. Siewleskiuk and J. Gorecki, *J. Phys. Chem. A* **106**, 4068 (2002).
- [11] K. Suzuki, T. Yoshinobu, and H. Iwasaki, *J. Phys. Chem. A* **104**, 5154 (2000).
- [12] A. F. Taylor, G. R. Armstrong, N. Goodchild, and S. K. Scott, *Phys. Chem. Chem. Phys.* **5**, 3928 (2003).
- [13] G. R. Armstrong, A. F. Taylor, S. K. Scott, and V. Gaspar, *Phys. Chem. Chem. Phys.* **6**, 4677 (2004).
- [14] A. B. Rovinsky and A. M. Zhabotinsky, *J. Phys. Chem.* **88**, 6081 (1984).
- [15] A. B. Rovinsky, *J. Phys. Chem.* **90**, 217 (1986).
- [16] J. Siewleskiuk and J. Gorecki, *J. Phys. Chem. A* **105**, 8189 (2001).
- [17] T. Kusumi, T. Yamaguchi, R. R. Aliev, T. Amemiya, T. Ohmori, H. Hashimoto, and K. Yoshikawa, *Chem. Phys. Lett.* **271**, 355 (1997).
- [18] A. Lazar, Z. Noszticzius, H-D. Forsterling, and Z. Nagy-Ungvrai, *Physica D* **84**, 112 (1995).
- [19] J. Gorecki, K. Yoshikawa, and Y. Igarashi, *J. Phys. Chem. A* **107**, 1664 (2003).
- [20] A. Toth, V. Gaspar, and K. Showalter, *J. Phys. Chem.* **98**, 522 (1994).